Angular momentum of fission fragments

G. F. Bertsch,[1] T. Kawano,[2] and L. M. Robledo[3]

[1]*Department of Physics and Institute of Nuclear Theory, University of Washington, Seattle, Washington 98915, USA*
[2]*Theoretical Division, Los Alamos National Laboratory, Los Alamos, New Mexico 87545, USA*
[3]*Departamento de Física Teórica, Universidad Autónoma de Madrid, 28049-Madrid, Spain*

The strong deformation present immediately after scission has consequences for the angular momentum population of the fragments as well as the angular distribution of their decay radiation. We find that the usual spin-cutoff parametrization describes very well the angular momentum distribution associated with the deformation of the fragments at the scission point. Depending on the deformation, its contribution can be comparable to the thermal contribution to the angular momentum of the newly formed fragments. The M distribution of the angular momentum is highly polarized and gives rise to large anisotropies in the subsequent γ cascade. We treat in detail a typical γ cascade in a daughter nucleus, following usual model assumptions except for the anisotropy of the initial state. In principle, the observed anisotropy can provide information on the relative amounts of deformation and thermal energy present at the scission point.

I. INTRODUCTION

Fission is a very complex nuclear reaction, both before and after the scission point. In principle the post-scission theory should be simpler because one is treating ordinary decay processes (γ and neutron emission) in nearly isolated midmass nuclei. However, there are differences from the decays of the excited nuclei produced in compound-nucleus reactions. Most importantly, the fission fragments may start in a state of high deformation aligned along the fission axis. Until recently [1], the angular momentum of the fragments as been treated statistically, ignoring the specific consequences of the deformation. Without inclusion of deformation effects, statistical modeling fails to reproduce average angular momenta by as much as a factor of two [2].

The goal of this paper is to calculate the effects of the deformation on the angular momentum distribution of the nascent fission fragments and their subsequent decay. The theory of the scission process is now under active development and many details are still obscure. One promising approach to determine properties of the fragments immediately following scission is time-dependent density functional theory [3] (see also Ref. [4]). The relation between deformation and angular momentum content can be reasonably modeled in well-established mean-field theories such as Hartree-Fock (HF) or Hartree-Fock-Bogoliubov (HFB). In the first section below, we estimate the average angular momentum in deformed configurations using one of the popular energy density functionals (Gogny D1S). In the section after that we determine the angular momentum probability distribution by projection. We find that the shape of the J distribution coming from deformation is nearly identical to the shape assumed in the statistical theory, differing only by the parameter controlling the average width $\langle J^2 \rangle$.

An interesting observable that has hardly been used in the past is the angular distribution of the decay γ rays. Due to the alignment of the deformed fragment along the fission axis, the M distribution of its states favors $M = 0$ along the axis. Here, we examine the angular distributions modeling the cascade from a fully aligned initial population. We find that the effect on the γ distribution can approach a factor of two in anisotropy. This effect is certainly measurable even in the presence of a large contribution from the isotropic quasiparticle contribution. The sign of the anisotropy is opposite for dipole and quadrupole photons, and in fact the both kinds of anisotropy have been seen in the final decays to the ground states of daughter nuclei [5].

Of course the angular momentum distribution also has contributions from quasiparticle excitations. Typically the pre-scission state is already highly excited above the collective potential energy surface and that excitation energy will be carried over to the post-scission fragments. The strong alignment of the deformed initial configuration is degraded by the presence of quasiparticles and both $\langle J^2 \rangle$ and the angular distributions will be affected. However, in view of all of the uncertainties in the present theory at the scission point we have not attempted to make a quantitative estimate of the resulting cascade angular distributions.

II. ANGULAR MOMENTUM OF ALIGNED DEFORMED NUCLEI

The deformation and alignment of the fission fragments requires that the wave function be a coherent superposition of angular momentum states. To determine the angular momentum content, we take the wave function from self-consistent mean-field theory. The first question we address is the relationship between deformation as characterized by the

Bohr parameter β and the average squared angular momentum $\langle J^2 \rangle$. The second question is how the angular momentum is distributed, i.e., the probability distribution $P(J)$ given its average for the configuration. These relationships were also studied in Ref. [1] using different modeling assumptions.

III. MEAN-SQUARE ANGULAR MOMENTUM

We construct deformed configurations using the Gogny D1S energy functional in the HF approximation, constraining on the mass quadrupole operator $Q_0 = \langle \Psi | 2z^2 - x^2 - y^2 | \Psi \rangle$. Here, the many-body wave function Ψ is a Slater determinant of orbitals. It is conventional to characterize the shape by the deformation parameter β defined as

$$\beta = \frac{(5\pi)^{1/2}}{3A^{5/3}r_0^2} Q_0, \tag{1}$$

where $r_0 = 1.2$ fm.

The general HF formula for the mean-square angular momentum $\langle J_i^2 \rangle$ around a Cartesian axis $i = x, y, z$ is $\langle \Psi | \hat{J}_i^2 | \Psi \rangle = \sum_{k,k'} n_k (1 - n_{k'}) \langle k | \hat{j}_i | k' \rangle^2$, where k, k' label a complete set of single-particle orbitals and n_k (equal to 0 or 1) is the occupation number in the wave function. A similar formula applies to HFB wave functions [[6], Eq. (49)], [[1], Eq. (40)].

We carry out the constrained minimization of the energy functional using the code HFB$_{\text{AXIAL}}$ written by one of us (L.M.R.). We consider several daughter nuclei that are prominent among the products of the ^{235}U(n, f) reaction, namely the light fragments ^{96}Kr, ^{96}Sr, and ^{96}Zr, and the heavy fragments ^{140}Te, ^{140}Xe, and ^{140}Ba. Since the scission dynamics is still obscure and different models can give very different shapes of the newly formed fission fragments, we do not attempt to calculate the deformations here but rather consider a range.

The output wave function of HFB$_{\text{AXIAL}}$ is axially symmetric and invariant under time reversal. This implies that the angular momentum satisfies $\langle J_z^2 \rangle = 0$ and $\langle J_x^2 \rangle = \langle J_y^2 \rangle$. The code's text output includes the expectation value $\langle J_x^2 \rangle$, from which we obtain $\langle J^2 \rangle = 2 \langle J_x^2 \rangle$. Graphs of $\langle J^2 \rangle_\beta$ are shown in Fig. 1 for the six nuclei mentioned in the previous paragraph. The curves are far from smooth, due to the strong shell effects in the HF approximation. As the deformation increases, particles jump to orbitals of higher angular momentum, discontinuously increasing the total. The dashed lines in the figure are visual fits assuming a linear relationship. A linear formula covering both sets of nuclei is[1,2]

$$\langle J^2 \rangle \approx (0.3 \pm 0.05) A^{3/2} \beta. \tag{2}$$

To assess the importance of the deformation contribution we can look to the existing theory on the scission dynamics. In one extreme, the scission is treated as a statistical process,
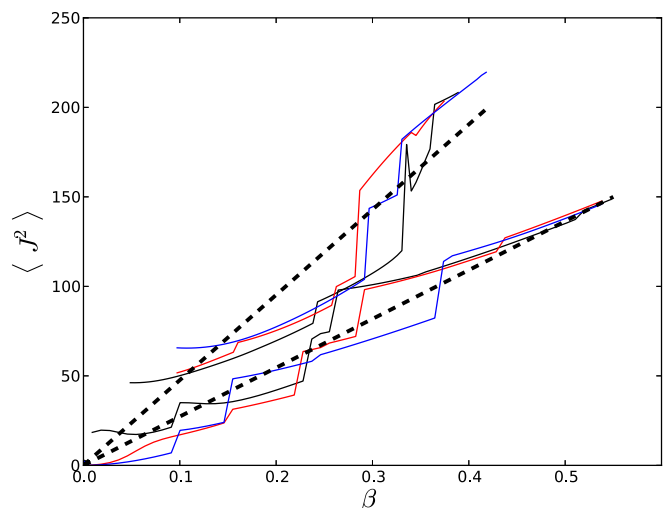
---

[1]Here and elsewhere, the angular momentum is given in units of $\hbar$.
[2]Equation (2) is purely phenomenological. It would be interesting to determine the leading dependence on A and β theoretically, perhaps using semiclassical methods.


FIG. 1. Angular momentum of various fission fragments as a function of deformation β. The upper black, blue, and red lines are for heavy fission fragments ^{140}Ba, ^{140}Te, and ^{140}Xe, respectively. The lower lines are The other source of angular momentum is the quasiparticle contribution; we hope to include its effects in a later publication.for the light fission fragments ^{96}Kr, ^{96}Zr, and ^{96}Sr. The dashed lines show the fit obtained with Eq. (1).

depending only on the density of states of the daughter fragments [7–9]. In particular, Ref. [8] concluded that the lighter fragment would be formed with a deformation $\beta \approx 0.6$. In the opposite extreme, the scission can now be treated without any statistical assumptions by time-dependent self-consistent mean field theory [3]. In Ref. [10] it was found that the deformation of the lighter post-scission fragment of mass $A = 105$ was in the range $\beta = 0.55$–0.7, depending on the energy functional. Applying Eq. (2), the coherent angular momentum would be in the range $\langle J^2 \rangle = 175$–$220$. This is much larger than the estimates ~ 100 based on statistical modeling [2]. We may conclude that the coherent deformation is potentially the most important contributor to the angular momentum of the final state. The other source of angular momentum is the quasiparticle contribution; we hope to include its effects in a later publication.

IV. J DISTRIBUTION

Next we analyze the distribution of angular momenta in the deformed wave function. An aligned axially symmetry wave function can be decomposed into angular momentum eigenstates $|JM\rangle$ as

$$|\Psi\rangle = \sum_J a_J |J0\rangle, \tag{3}$$

where $\sum_J |a_J|^2 = 1$, and J is restricted to even angular momenta for an even-even nucleus in its ground state. The individual probabilities $|a_J|^2$ can be calculated by the projection formula

$$|a_J|^2 = (2J + 1) \int_0^1 d\mu \langle \Psi | \hat{R}(\theta) | \Psi \rangle P_J(\mu), \tag{4}$$
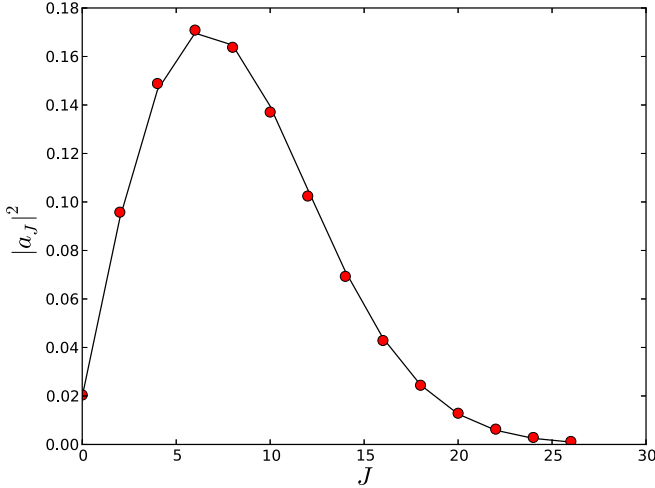
FIG. 2. Angular momentum decomposition of a axially deformed wave function aligned along the z axis. Black: Eq. (6); red circles: Eq. (5).

where $\hat{R}$ is the rotation operator about the x axis, $\mu = \cos\theta$, and P_J is a Legendre polynomial. In practice [11,12], the overlap $\langle \Psi | \hat{R}(\theta) | \Psi \rangle$ is very well fitted by an exponential function of μ. Then the probabilities $|a_J|^2$ are computed from the integral

$$|a_J|^2 = (2J + 1) \int_0^1 d\mu\, e^{-C(1-\mu^2)} P_J(\mu). \quad (5)$$

Here, C is a constant determined from $\langle J^2 \rangle = \sum_J J(J+1)|a_J|^2$; it is approximately given by $D \approx \langle J^2 \rangle/4$. The resulting distribution for mean square angular momentum $\langle J_p^2 \rangle = \langle J^2 \rangle = 100$ is shown by the red circles in Fig. 2.

In statistical theory, the angular momentum distribution is often parametrized by Gaussians in the three Cartesian directions, $P(J_i) \sim e^{-J_i^2/2\langle J_i^2 \rangle}$. Assuming this functional form for the aligned intrinsic state and adding a quantum correction, we obtain the standard spin-cutoff formula [[5], Eq. (3)]

$$|a_J|^2 \sim (J + 1/2) e^{-J(J+1)/2\sigma^2}, \quad (6)$$

where $\sigma^2 \approx \sum_i \langle J_i^2 \rangle$. This distribution is shown by the black line in Fig. 2. We see that Eq. (6) is an excellent approximation to the projection formula Eq. (5).

In fact, the same formula Eq. (6) emerges from the semiclassical limit of a Gaussian distribution only in the transverse directions [1]. We note also that Refs. [13,14] also assume that the angular momentum is purely transverse.

V. STATISTICAL DECAY ANGULAR DISTRIBUTIONS

The γ-ray angular distribution from fission products carries information about the alignment of the deformed fragments. Indeed, significant anisotropies with respect to the fission axis were observed a long time ago [5]. There will also be a component due to the Doppler shifts which we ignore here.

In the γ decay $J' \rightarrow J$ the relative populations of daughter states $\rho(J, M)$ are given in terms of the feeding population

distribution $\rho(J', M')$ as

$$\rho(J, M) = \sum_{M'} \rho(J'M')(J'M'LM{-}M'|JM)^2. \quad (7)$$

Here, L is the multipolarity of the electromagnetic transition and $(J'M'LM - M'|JM)$ is a Clebsch-Gordan coefficient. The angular distribution $p(\theta)$ of the emitted photon is given by [15]

$$p(\theta) = N_J \sum_{M',M,K} \left| d_{K,1}^L(\theta) \right|^2 \rho(J'M')(J'M'LK|JM)^2, \quad (8)$$

where $d_{\mu,\mu'}^L$ is the reduced Wigner $\mathcal{D}$ function and N_J is a normalization constant.

We first analyze a very simple cascade that starts from a pure aligned state of angular momentum $(J, M) = (7, 0)$. The cascade proceeds by emitting dipole photons until the final transition which is quadrupolar. Each dipole decay lowers J by one unit until the final quadrupole decay. Thus the decay chain is $7 \rightarrow 6 \rightarrow 5 \rightarrow 4 \rightarrow 3 \rightarrow 2 \rightarrow 0$. The population of the 2^+ first excited state remain highly polarized despite the 4–5 preceding γ decays, as may be seen in as the solid line in the upper panel of Fig. 3. The angular distribution of the subsequent quadrupolar γ ray is shown in the lower panel of the figure. It has an easily measurable anisotropy and is peaked along the fission axis.

The dipole photons in the cascade also show an anisotropy. The top panel of Fig. 4 shows the distribution of dipole photons with respect to their angular momentum about the fission axis. One sees that $M = 0$ is favored even though $M = \pm 1$ is permitted for the great majority of the transitions in the cascade. Again the resulting angular distribution (shown in the bottom panel of the figure) is anisotropic, but now suppressing emission along the fission axis.

We have confirmed these findings with a more realistic treatment of the level spectrum in the cascade. The level density is generated stochastically following the constant-temperature formula [16,17] $\rho(E^*) = \exp(-E^*/T)/T$, where E^* is the excitation energy and the parameter T is set to 1 MeV. Each level is assigned randomly an angular momentum and parity J^π, except as described below. The probability distribution for J is given by the spin-cutoff formula Eq. (6). Here, we assume that the factor σ depends on excitation energy E^* as [18] $\sigma = b(E^*)^{1/4}$ with the parameter $b = 4 \text{ MeV}^{-1/4}$. The stochastic spectrum is modified in two ways. First, the lowest two states are given spin-parity assignments 0^+ and 2^+, typical of nearly all even-even nuclei. We also limit the maximum $J = J_{\max}$ in the probabilistic determination to ensure the cascade will not end on an isomeric state.

The decay branching is also treated stochastically assuming that all transitions except the final one are electric dipole in character, with relative transition rates given by the Brink-Axel strength function [19]

$$T_\gamma \propto E_\gamma^3 \Gamma \frac{E_\gamma \Gamma}{\left(E_R^2 - E_\gamma^2\right)^2 + E_\gamma^2 \Gamma^2}. \quad (9)$$

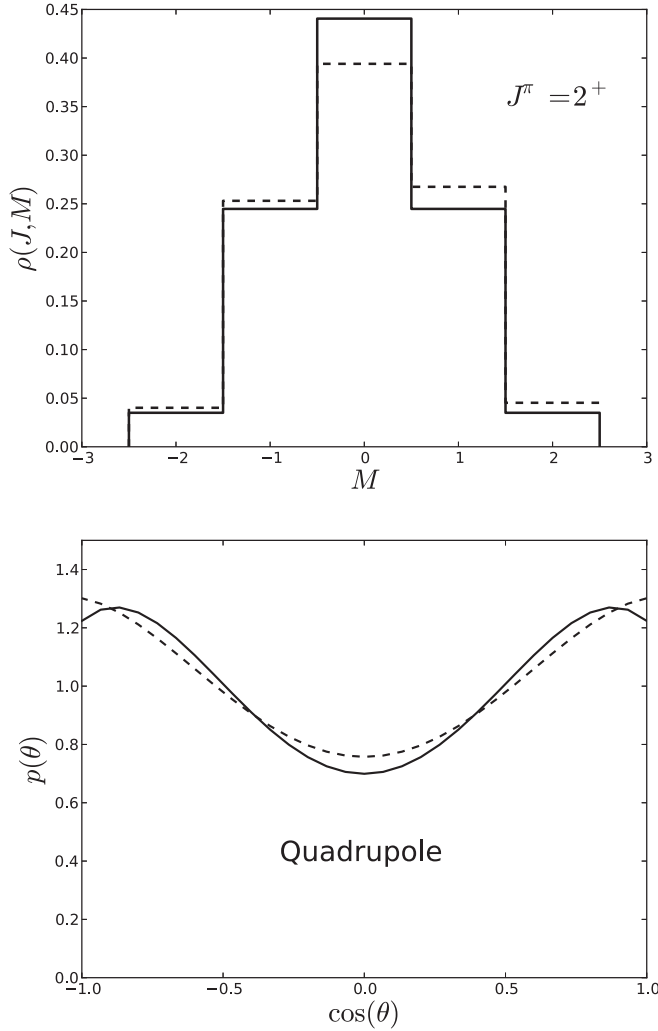The giant resonance parameters are taken as $\Gamma = 5$ MeV and $E_R = 15$ MeV.

FIG. 3. Top panel: histogram of M-state populations of the 2^+ first excited level in the cascade. Solid line is from the simplified cascade $7 \to 6 \to 5 \to 4 \to 3 \to 2$ starting from the initial distribution $\rho(7, M) = \delta_{M0}$. Dashed line is from the realistic cascade (see text). Bottom panel: resulting angular distribution of the γ decay $2^+ \to 0^+_{\text{g.s.}}$.
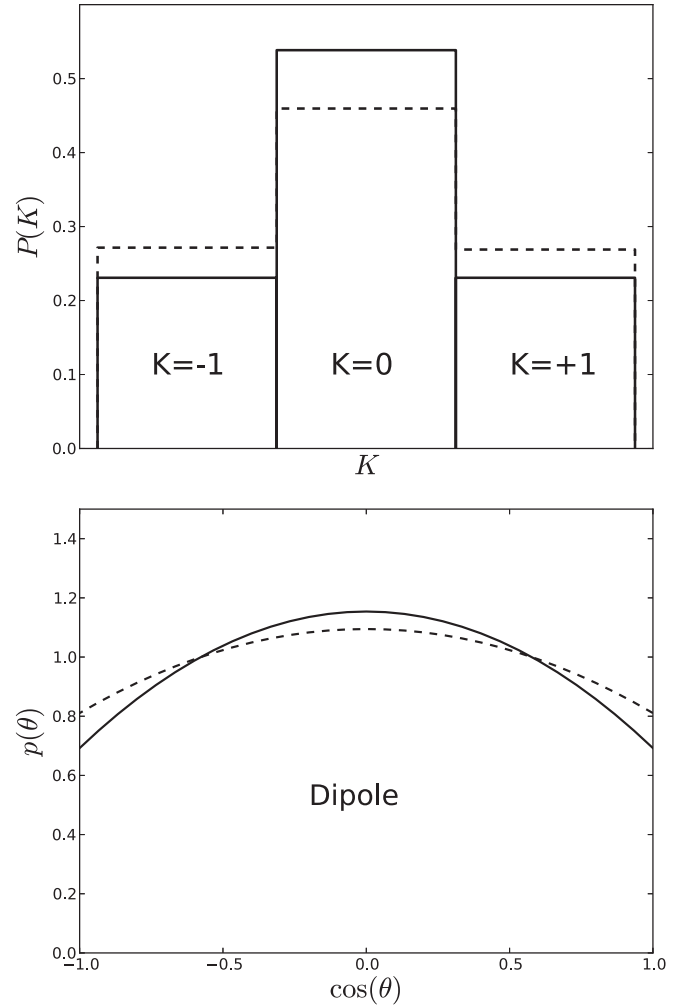

FIG. 4. Top panel: Dipole γ probabilities as a function of K of the γ. Solid histogram is from the simplified cascade; dashed line is from the realistic cascade. Bottom panel: Dipole γ angular distribution.

The angular momentum of the entry point is taken as $(J, M) = (8, 0)$, chosen to be close to average values obtained from phenomenological analyses [20,21]. Its excitation energy should be a little higher than the neutron separation energy; we set it to $E^* = 8$ MeV. Further details are given in the Supplemental Material [22].

The resulting populations of M quantum numbers and γ angular distributions are shown as the dashed lines in Figs. 3 and 4. We see that the qualitative character of the polarization remain in the more realistic treatment. It is common to characterize the anisotropy as coefficients of Legendre polynomials,

$$p(\theta) = 1 + c_2 P_2(\cos \theta) + \ldots . \quad (10)$$

The results of our models are shown in Table I. For the realistic cascade, we found $c_2 = -0.2$ and 0.4 for the dipole and quadrupole distributions, respectively.

The qualitative features of the γ decay angular distribution were already seen many years ago [5] in a study of the decay products from the spontaneous fission of ^{252}Cf. Measurements were presented for transitions from the first excited state to the ground state in the isotopes ^{144}Ba, ^{110}Ru, and ^{105}Mo; the measured anisotropy coefficients were $c_2 \approx 0.1, 0.3$, and -0.3, respectively. The first two are electric quadrupole transitions and the signs agree with expectations, as was indeed noted in the paper. The higher anisotropy suggests that heavier fragment is more spherical, also expected due to its proximity to the doubly magic ^{132}Sn. The negative c_2 for ^{105}Mo was left unexplained in the paper. We now know that spin-parity assignments of the ground and first excited states in that nucleus [23]: the transition is $7/2^- \to 5/2^-$ and has a predominantly $M1$ character. Thus, we expect a dipole anisotropy, as observed. Overall, the large amplitudes of the measured anisotropies suggest that quasiparticle excitations do not dominate the angular momentum distribution of the newly formed fragments.

TABLE I. Anisotropy coefficients c_2 in Eq. (10). The model labeled "simple" assumes the decay chain having five stretched dipole transitions followed by a single quadrupole transition to the ground state. The model labeled "realistic" is based on the phenomenological level densities and dipole strength function described in the text. The experimental anisotropies are for the decays from the first excited state to the ground state reported in Ref. [5].

Model	Dipole	Quadrupole
Simple	−0.3	0.4
Realistic	−0.2	0.4
Exp. ^{144}Ba		0.1
Exp. ^{110}Ru		0.3
Exp. ^{105}Mo	−0.3	

VI. OUTLOOK

We hope that the observable discussed here, the prompt γ angular distribution, can be used to learn more about the division of excitation energy in the newly formed fission fragments. Unfortunately, there are too many variables to make a direct connection. The amount of deformation at scission, and its energy cost, is still very much uncertain. We believe that much of the excitation energy in the newly formed fission fragments is thermal, in the form of quasiparticle excitations, but we are still lacking a theory of the scission process that can describe the sharing of thermal excitation energy between the two fragments. Combining quasiparticle angular momentum with the deformation will certainly reduce the anisotropy of the gamma radiation, and that relationship needs to be understood quantitatively.

Another question that needs to be re-examined is the role of Coulomb excitation in the post-scission acceleration phase. Both dipole and quadrupole components of the Coulomb field of the partner fragment are large in first hundred femtoseconds after scission. Reference [[5], Appendix] found the effects to be small in a simple model, but with present-day theoretical tools one could make a much more reliable estimate.

[1] L. Bonneau, P. Quentin, and I. N. Mikhailov, Phys. Rev. C **75**, 064313 (2007).

[2] I. Stetcu, P. Talou, T. Kawano, and M. Jandel, Phys. Rev. C **90**, 024617 (2014).

[3] A. Bulgac, P. Magierski, K. Roche, and I. Stetcu, Phys. Rev. Lett. **116**, 122504 (2015).

[4] G. F. Bertsch, W. Younes, and L. M. Robledo, Phys. Rev. C **97**, 064619 (2018).

[5] J. B. Wihelmy, E. Cheifetz, R. C. Jared *et al.*, Phys. Rev. C **5**, 2041 (1972).

[6] Y. Alhassid, G. F. Bertsch, C. N. Gilbreth, and H. Nakada, Phys. Rev. C **93**, 044320 (2016).

[7] P. Fong, *Statistical Theory of Nuclear Fission* (Gordon and Breach, New York, 1969).

[8] B. D. Wilkins, Phys. Rev. C **14**, 1832 (1976).

[9] J.-F. Lemaitre, S. Panebianco, J.-L. Sida, and S. Hilaire, Phys. Rev. C **92**, 034617 (2015).

[10] A. Bulgac, S. Jin, K. Roche, N. Schunck, and I. Stetcu, arXiv:1806.00694.

[11] K. Hagino, P.-G. Reinhard, and G. F. Bertsch, Phys. Rev. C **65**, 064320 (2002).

[12] M. Bender, G. F. Bertsch, and P.-H. Heenen, Phys. Rev. C **69**, 034340 (2004).

[13] R. Vogt and J. Randrup, Phys. Rev. C **87**, 044602 (2013).

[14] J. Randrup and R. Vogt, Phys. Rev. C **89**, 044601 (2014).

[15] A. deShalit and H. Feshbach, *Theoretical Nuclear Physics: Nuclear Structure* (Wiley, New York, 1974), Eq. (5.13).

[16] A. Gilbert and A. Cameron, Can. J. Phys. **43**, 1446 (1965).

[17] B. Becker, P. Talou, T. Kawano, Y. Danon, and I. Stetcu, Phys. Rev. C **87**, 014617 (2013).

[18] S. Okumura, T. Kawano, P. Jaffke, P. Talou, and S. Chiba, J. Nucl. Sci. Technol. **55**, 1009 (2018).

[19] R. Capote *et al.*, Nucl. Data Sheets **110**, 3107 (2009).

[20] H. Naik, S. P. Dange, and R. J. Singh, Phys. Rev. C **71**, 014304 (2005)

[21] O. Litaize and O. Serot, Phys. Rev. C **82**, 054616 (2010).

[22] See Supplemental Material at http://link.aps.org/supplemental/10.1103/PhysRevC.99.034603 for the script calculating the M populations in the cascade and the angular distribution of γ rays.

[23] National Nuclear Data Center nndc.bnl.gov/nudat2/.